

## 微调镝(III)离子配位环境提升单离子磁体有效能垒

ALI Basharat<sup>1,2</sup> 李晓磊<sup>1</sup> 唐金魁<sup>\*,1,2</sup>

(<sup>1</sup>中国科学院长春应用化学研究所, 稀土资源利用国家重点实验室, 长春 130022)

(<sup>2</sup>中国科学技术大学应用化学与工程学院, 合肥 230026)

**摘要:** 对于合成化学家来说, 通过合成策略调控单离子磁体的磁动力学是一项艰巨的任务。我们以三(2-羟基亚苄基)三氨基胍配体(L)合成了2例单核Dy(III)配合物[Dy(L)<sub>2</sub>(H<sub>2</sub>O)<sub>2</sub>](ClO<sub>4</sub>)·2H<sub>2</sub>O·2CH<sub>3</sub>CN·CH<sub>3</sub>OH (**1**)和[Dy(L)<sub>2</sub>(H<sub>2</sub>O)<sub>2</sub>](CF<sub>3</sub>SO<sub>3</sub>)·4H<sub>2</sub>O·2CH<sub>3</sub>OH (**2**)。对其结构和磁性研究表明, 不同的抗衡阴离子对于配合物**1**和**2**的动态磁行为有显著影响。2个配合物中, Dy(III)中心都具有三角十二面体D<sub>2d</sub>对称性, 在零直流场下表现出单离子磁体的行为, 其有效能垒分别为358 K (**1**)和309 K (**2**)。结构参数对比表明轴向位置的键长和键角微小变化对轴向配体场产生了显著的影响, 而轴向配体场的微小变化导致了2个配合物交流磁性的差异。

**关键词:** 镝; 配合物; 磁性; 单分子磁体

中图分类号: O614.342

文献标识码: A

文章编号: 1001-4861(2021)08-1519-08

DOI: 10.11862/CJIC.2021.174

## Improving Energy Barrier by Altering Coordination Environment in Two Dy(III) Single-Ion Magnets

ALI Basharat<sup>1,2</sup> LI Xiao-Lei<sup>1</sup> TANG Jin-Kui<sup>\*,1,2</sup>

(<sup>1</sup>State Key Laboratory of Rare Earth Resource Utilization, Changchun Institute of Applied Chemistry,  
Chinese Academy of Sciences, Changchun 130022, China)

(<sup>2</sup>School of Applied Chemistry and Engineering, University of Science and Technology of China, Hefei 230026, China)

**Abstract:** Altering the synthetic strategies and further tuning the magnetic dynamics of single-ion magnets (SIMs) are critical tasks for chemists. Two mononuclear Dy(III) complexes [DyL<sub>2</sub>(H<sub>2</sub>O)<sub>2</sub>](ClO<sub>4</sub>)·2H<sub>2</sub>O·2CH<sub>3</sub>CN·CH<sub>3</sub>OH (**1**) and [DyL<sub>2</sub>(H<sub>2</sub>O)<sub>2</sub>](CF<sub>3</sub>SO<sub>3</sub>)·4H<sub>2</sub>O·2CH<sub>3</sub>OH (**2**) have been successfully synthesized by using tris(2-hydroxybenzylidene)tri-aminoguanidine ligand (L). Structural and magnetic investigations reveal that different counter anions play an important role in dynamic magnetic behaviors of **1** and **2**. In both the complexes the Dy(III) centers are eight-coordinated with triangular dodecahedron D<sub>2d</sub> symmetry. They all showed single-ion magnets (SIMs) behavior under zero dc applied field with effective energy barriers (*U*<sub>eff</sub>) of 358 K (**1**) and 309 K (**2**), respectively. A comparison of the structural parameters shows that the small but significant changes at axial positions in bond lengths and bond angles affect the axial ligand field which in turn is mainly responsible for distinct magnetic properties of both the complexes. CCDC: 2064802, **1**; 2064803, **2**.

**Keywords:** dysprosium; coordination compounds; magnetism; single-molecule magnets

收稿日期: 2021-05-08。收修改稿日期: 2021-06-25。

国家自然科学基金(No.21871247, 21801237)、吉林省自然科学基金(No.20200201244JC)和中国科学院基础前沿科学研究计划(No. ZDBS-LY-SLH023)资助。

\*通信联系人。E-mail: tang@ciac.ac.cn

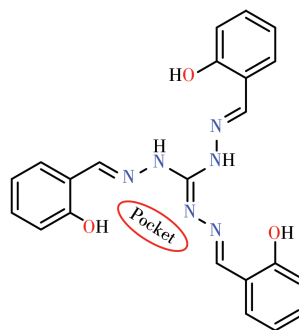
## 0 Introduction

Single-molecule magnets (SMMs), which are complexes presenting slow relaxation of magnetization below certain temperatures, offer the fascinating possibility of constructing switchable, molecular-based devices that manipulate or store information on tuning their molecular spin<sup>[1-2]</sup>. Furthermore, owing to their possible applications in high - density data storage devices, spintronics and quantum computing, SMMs have become one of the most broadly studied fields among coordination compounds<sup>[1,3-6]</sup>. Even though thousands of SMMs with distinct topologies and magnetic properties have been described by the researchers worldwide, SMMs are still far from practical implementations<sup>[7-13]</sup>. Fortunately, very recently the scientists have greatly succeeded to set the new records for effective energy barrier ( $U_{\text{eff}}$ ) and blocking temperature ( $T_{\text{B}}$ ) on lanthanide - based single - ion magnets (SIMs). For example, SIMs of pentagonal bipyramidal geometries were designed systematically by using weak equatorial ligands and strong axial ligands<sup>[14-16]</sup> and consequently, the highest  $U_{\text{eff}}$  of 2 217 K with a record  $T_{\text{B}}$  of 80 K has been achieved<sup>[14]</sup>.

Earlier, it was believed that the most suitable strategy to improve the performance of SMMs was to enhance the spin value of the ground state. Soon it was realized that the single-ion magnetic anisotropy is often canceled out within the molecule which gives a weak magnetic anisotropy and results in a small  $U_{\text{eff}}$  for the whole system<sup>[17]</sup>. Alternatively, the mononuclear SIMs, containing only one spin center, allows the scientists to explore and switch the single-ion magnetic anisotropy. Furthermore, it is well-known that the coordination environment of the target compound is usually perturbed through rational changes in synthetic strategies such as pH value, solvent effect, electrostatic potential, or the counter anions around the central metal ion in order to enhance or reduce the electron density<sup>[18-21]</sup>. The particular concern here is the tunable counter anions effect that usually brings microenvironment differences in the geometric symmetry which in turn display dynamic SMMs behaviors<sup>[22]</sup>.

The coordination chemistry of transition metals

based on triaminoguanidine ligands has already been well established<sup>[23-33]</sup>. Very recently, the researchers have also started to explore interesting magnetic properties of 3d transition metal complexes carrying rigid triaminoguanidine-backbones<sup>[34-44]</sup>. Surprisingly, the magnetochemistry of such ligands with 4f rare earth metals have never been explored before, except only one study that also belongs to our group, where we have expressed a family of Dy(III)-SIMs associated with guanidine-based ligands in which the effect of coordinated solvents and lattice counter anions simultaneously<sup>[45]</sup>. To the extension of our previous work, we now have succeeded to synthesize two mononuclear Dy(III)-SIMs by using triaminoguanidine-based ligand L (L=tris(2-hydroxybenzylidene)triaminoguanidine) (Scheme 1) having formulas  $[\text{DyL}_2(\text{H}_2\text{O})_2]\text{ClO}_4 \cdot 2\text{H}_2\text{O} \cdot 2\text{CH}_3\text{CN} \cdot \text{CH}_3\text{OH}$  (**1**) and  $[\text{DyL}_2(\text{H}_2\text{O})_2]\text{CF}_3\text{SO}_3 \cdot 4\text{H}_2\text{O} \cdot 2\text{CH}_3\text{OH}$  (**2**) with different counter anions. Interestingly, structural and magnetic studies reveal that different counter anions bring small but significant changes in bond lengths and bond angles and affect the axial ligand field which consequently exhibited dynamic single-molecule magnetic relaxation behaviors with  $U_{\text{eff}}$  of 358 K (**1**), and 309 K (**2**), respectively, in the absence of a static magnetic field.



Scheme 1 Structural drawing of used ligand along with coordinating pocket

## 1 Experimental

### 1.1 Materials and methods

All solvents and chemicals were obtained from commercial sources of analytical grade and were used as received. Ligand L was synthesized according to the procedure reported in the literature<sup>[29,46-47]</sup>. Elemental analyses for C, H and N were performed on a Perkin-

Elmer 2400 analyzer. Magnetic measurements were done on the polycrystalline sample with a Quantum Design MPMS-XL7 SQUID magnetometer from 1.9~300 K temperature range equipped with a 7 T magnet. Alternating-current (ac) measurements were obtained at 3.0 Oe with oscillating frequencies from 1~1 000 Hz and direct-current (dc) measurements were measured within 1.9~300 K temperature range with an external magnetic field of 1 000 Oe. The experimental magnetic susceptibility data were corrected for the diamagnetism contribution of all the atoms estimated from Pascal's tables and sample-holder calibration<sup>[48]</sup>.

### 1.1.1 Synthesis of complexes **1** and **2**

Dy(ClO<sub>4</sub>)<sub>3</sub>·6H<sub>2</sub>O (0.10 mmol) and ligand **L** (0.20 mmol) were dissolved in a 20 mL mixture of methanol and acetonitrile (1:1, V/V) followed by triethylamine (0.20 mmol). After 3 h of stirring at room temperature, the resultant solution was filtered and put aside for slow evaporation. Well sized yellow color block-like crystals suitable for single crystal measurements were collected after a couple of days. Complex **2** was also obtained by using a similar procedure as for **1**, by replacing Dy(ClO<sub>4</sub>)<sub>3</sub>·6H<sub>2</sub>O with Dy(SO<sub>3</sub>CF<sub>3</sub>)<sub>3</sub>·6H<sub>2</sub>O, respectively (Yield: ~70%, based on dysprosium for both the complexes).

Elemental Anal. Calcd. for C<sub>49</sub>H<sub>56</sub>ClDyN<sub>14</sub>O<sub>15</sub> (**1**, %): C, 46.01; H, 4.41; N, 15.33. Found(%): C, 45.97; H, 4.43; N, 15.31.

Elemental Anal. Calcd. for C<sub>47</sub>H<sub>58</sub>DyF<sub>3</sub>N<sub>12</sub>O<sub>17</sub>S (**2**, %): C, 42.94; H, 4.44; N, 12.79. Found(%): C, 43.16; H, 4.03; N, 12.82.

## 1.2 Crystallography

Single crystals of **1** and **2** were mounted on glass fibers under a microscope, and diffraction data were collected at corresponding temperatures (Table S1, Supporting information) using a Bruker AXS D8 Venture single-crystal diffractometer equipped with graphite-monochromatized (Cu K $\alpha$   $\lambda$ =0.154 178 nm (**1**), Mo K $\alpha$   $\lambda$ =0.071 073 nm (**2**)) in liquid N<sub>2</sub>. The molecular structures and mean plane analysis were designed from the DIAMOND (version 3.1). The structures were solved by SHELXT (direct methods) and refined by SHELXL (full-matrix least-squares tech-

niques) based on  $F^2$  in the Olex2 package<sup>[49-50]</sup>. Crystallographic data, structural refinement parameters and selected bond lengths and angles are given in Table S1~S3.

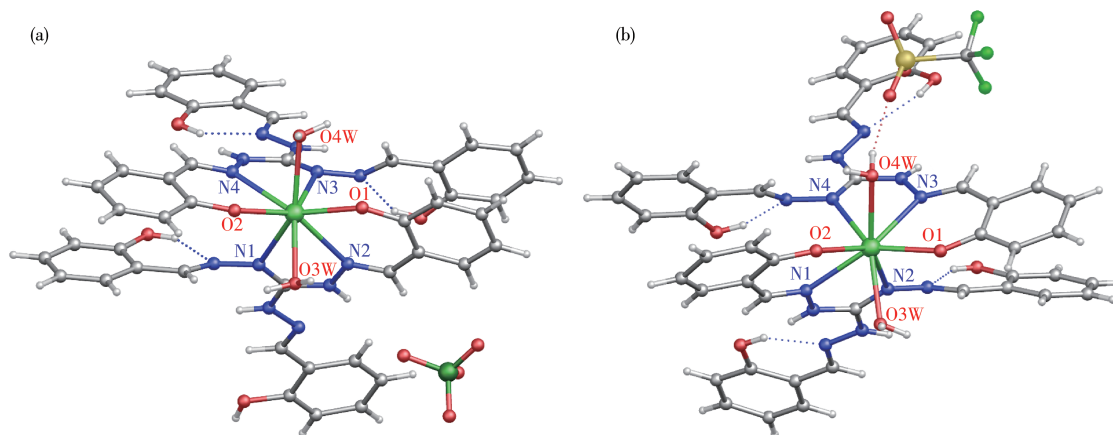
CCDC: 2064802, **1**; 2064803, **2**.

## 2 Results and discussion

### 2.1 Synthesis and structural description

Complexes **1** and **2** were prepared by reacting ligand **L** (0.20 mmol) with Dy(ClO<sub>4</sub>)<sub>3</sub>·6H<sub>2</sub>O and Dy(SO<sub>3</sub>CF<sub>3</sub>)<sub>3</sub>·6H<sub>2</sub>O (0.10 mmol), respectively in the presence of triethylamine (0.20 mmol) in a 20 mL mixture of methanol and acetonitrile (1:1, V/V). Single crystal X-ray diffraction analyses reveal that complexes **1** and **2** crystallize in monoclinic  $C2/c$  and triclinic  $P\bar{1}$  space group, respectively (Table S1).

Complexes **1** and **2** display similar coordination environments (Fig. 1), only differ in counter anion (ClO<sub>4</sub><sup>-</sup> for **1**; SO<sub>3</sub>CF<sub>3</sub><sup>-</sup> for **2**) along with some solvent molecules (CH<sub>3</sub>OH, 2CH<sub>3</sub>CN, 2H<sub>2</sub>O for **1** and 2CH<sub>3</sub>OH, 4H<sub>2</sub>O for **2**), respectively. Both compounds are octa-coordinated, six coordination sites (2NNO) from two singly deprotonated ligands and two O donors from two water molecules to complete the coordination sphere along with some solvent molecules in the lattice. The continuous shape measurements<sup>[51-53]</sup> indicate that geometry for both the complexes can be best described as triangular dodecahedron  $D_{2d}$  giving the values of 0.739 and 0.915 for **1** and **2**, respectively (Fig. S1, Table S2). The Dy1—O1 and Dy1—O2 bond lengths are 0.223 3(3), 0.222 3(3) nm and 0.222 51(3), 0.221 9(3) nm; Dy1—O3w and Dy1—O4w distances are 0.240 9(3), 0.246 7(3) nm and 0.241 1(3), 0.241 8(3) nm for **1** and **2**. Whereas the Dy—N bond distances fall in 0.246 2(4)~0.255 0(4) nm and 0.249 1(3)~0.243(3) nm of **1** and **2** (Table S3), respectively. The axial angles for both the complexes governed by coordinating deprotonated phenolic group of two ligands (O1—Dy1—O2) are 118.29(11)° and 115.26(11)°, respectively. The angles among O3w—Dy1—O4w are 129.77(11)° for **1** and 135.83(10)° for **2** (Table S4). Furthermore, the 3D molecular packing of both the complexes is also different, showing slight differences in intermolecular



Color codes: Dy, light green; C, gray; O, red; Cl, dark green; N, blue; F, bright green; S, yellow; Lattice solvent molecules are omitted for clarity

Fig.1 Molecular structures of **1** (a) and **2** (b)

Dy $\cdots$ Dy interactions along *a*, *b* and *c* axes, caused by different counter anions and some solvent molecules at special positions in the crystal lattice. The closest intermolecular distances of Dy $\cdots$ Dy ions are 0.603 nm for **1** and 0.582 nm for **2**, respectively (Fig. S2 and S3). These minor differences of bond lengths and bond angles along with diverse 3D molecular packing of complexes **1** and **2** induced by different counter anions/solvent molecules which in turn affect the anisotropy axes and are mainly responsible for their distinct magnetic properties<sup>[45]</sup>.

## 2.2 Magnetic properties

The dc magnetic susceptibility ( $\chi_M T$ ) experiments were performed on polycrystalline samples for both the complexes in a temperature range of 1.9~300 K in an applied field of 1 kOe (Fig. 2). The measured  $\chi_M T$  values at room temperature were 14.18 and 13.99 cm<sup>3</sup>·K·mol<sup>-1</sup> for complexes **1** and **2**, respectively, which were both well consistent with the expected value of 14.17 cm<sup>3</sup>·K·mol<sup>-1</sup> for a free Dy(III) ion ( $S=5/2$ ,  $L=5$ ,  $g=4/3$  and  $^6H_{15/2}$ ). Upon cooling, the  $\chi_M T$  values decreased gradually until 20 K, and then decreased rapidly, reaching 9.59 and 9.47 cm<sup>3</sup>·K·mol<sup>-1</sup> at 1.9 K, respectively. The decrease in the  $\chi_M T$  value in both the complexes is due to crystal field splitting, mainly the thermal depopulation of the Dy(III) Stark sublevels and/or weak intra/intermolecular interactions<sup>[54-57]</sup>. Comparatively, the  $\chi_M T$  curves for both the complexes were slightly different at low temperatures, very similar to recently reported analogous Dy(III) - SIMs<sup>[45]</sup> which can

be attributed to different intermolecular Dy $\cdots$ Dy distances, causing distinct antiferromagnetic dipole-dipole interactions among the molecules.

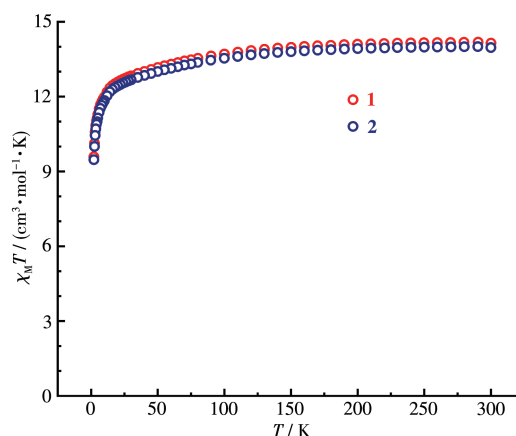


Fig.2 Temperature dependence of  $\chi_M T$  values of **1** and **2** under 1 kOe dc field

The field-dependent magnetization ( $M$  vs  $H$ ) of **1** and **2** were examined at 1.9~5.0 K in the field range of 0~70 kOe (Fig. S4). The maxima of magnetization for both the complexes were 5.87 $\mu_B$  and 5.58 $\mu_B$ , respectively. These experimental values were well lower than the expected saturation value of 10 $\mu_B$  for one uncorrelated Dy(III) ion, but agreed with the mean value of 5 $\mu_B$  under considerable crystal field, which imply a well-isolated ground Kramers doublet state. Further, non-superimposed  $M$  vs  $HT^{-1}$  (Inset of Fig. S4) and lack of saturation of  $M$  vs  $H$  plots at different temperatures indicating significant magnetic anisotropy<sup>[54-58]</sup>. Another important tool of the magnetic bi-stability is magnetic hysteresis which was experimentally measured for both

the complexes. Interestingly, both the complexes displayed well defined butterfly-shaped hysteresis loops at 1.9 K (Fig.S5).

The in-phase ( $\chi'$ ) and the out-of-phase ( $\chi''$ ) ac magnetic susceptibility measurements as a function of the frequency of **1** and **2** were performed under a zero dc field with a small ac field of 3 Oe. The frequency dependence  $\chi'$  and  $\chi''$  magnetic susceptibilities showed typical SMM behaviors for **1** and **2** (Fig.3 and S6). Both the complexes revealed a series of well-defined  $\chi''$  maxima in a temperature range of 9~24 K for **1** and 5~22 K for **2**, respectively. As seen from Fig. S7, another increase of the ac response was observed in the low-temperature region (below 9 K for **1** and 5 K for **2**), probably indicating the onset of pure quantum

tunneling<sup>[59]</sup>.

The Cole-Cole fitting graphs (Fig.4) of **1** and **2**, based on frequency-dependent data with the generalized Debye model<sup>[54-58]</sup> show nonsymmetrical semicircles. The obtained parameters are in the range of 0.024~0.3 (9~24 K) for **1** and 0.055~0.18 (5~22 K) for **2** respectively, giving a narrow distribution of relaxation times ( $\tau$ ) (Table S5 and S6). The Arrhenius plots ( $\ln \tau$  vs  $T^{-1}$ , Fig.5) were fitted considering the Orbach and Raman process to obtain the corresponding effective energy barrier of relaxation  $U_{\text{eff}}=358.18$  K ( $\tau_0=2.27\times 10^{-11}$  s) for **1** and  $U_{\text{eff}}=309.19$  K ( $\tau_0=2.64\times 10^{-9}$  s) for **2**<sup>[55]</sup>. The insets of Fig.5 shows the detail for the corresponding extracted parameters for both the complexes.

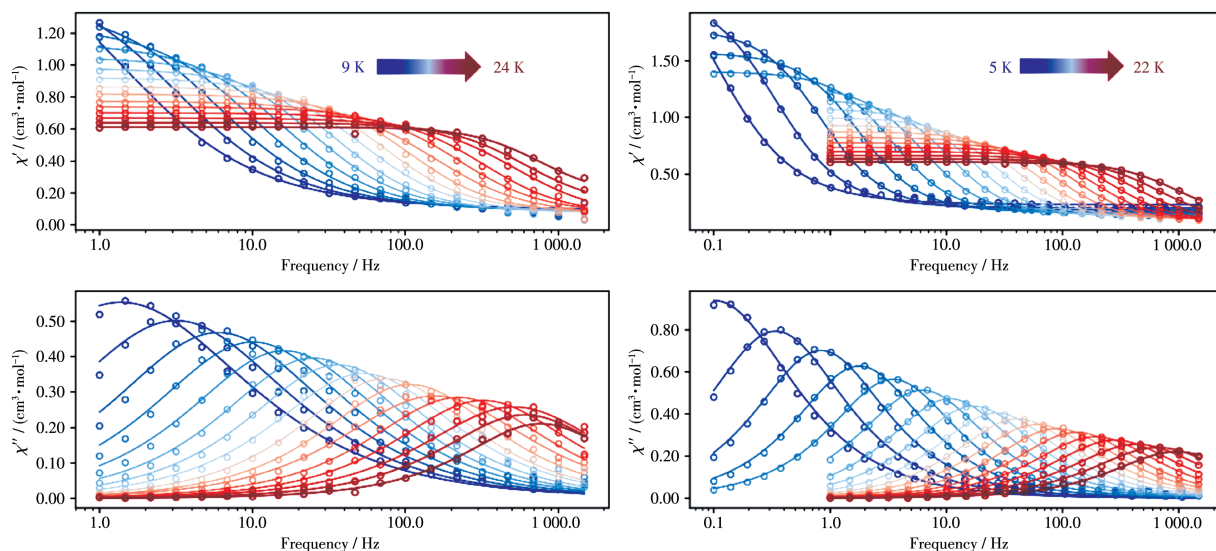


Fig.3 Frequency dependence of in-phase ( $\chi'$ ) and out-of-phase ( $\chi''$ ) plots of **1** (left) and **2** (right)

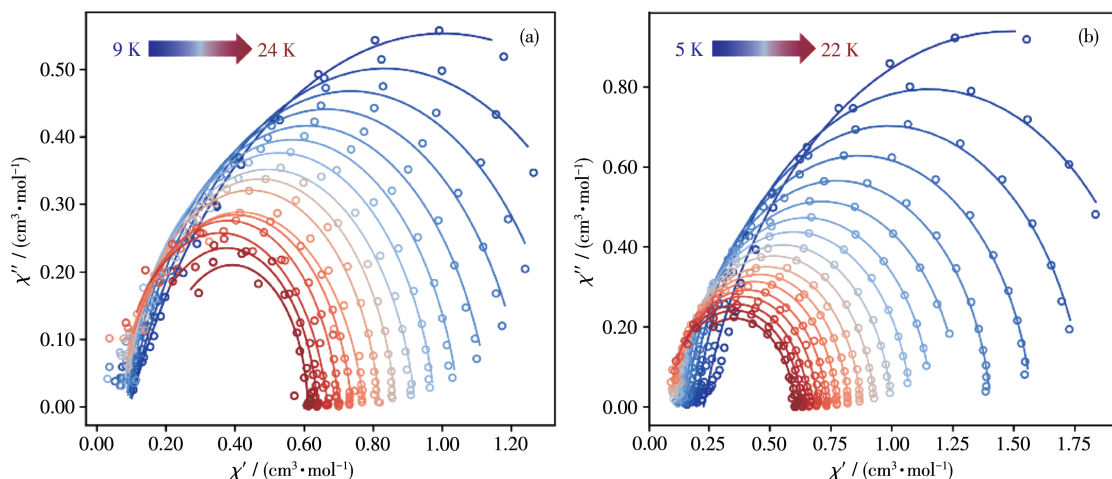
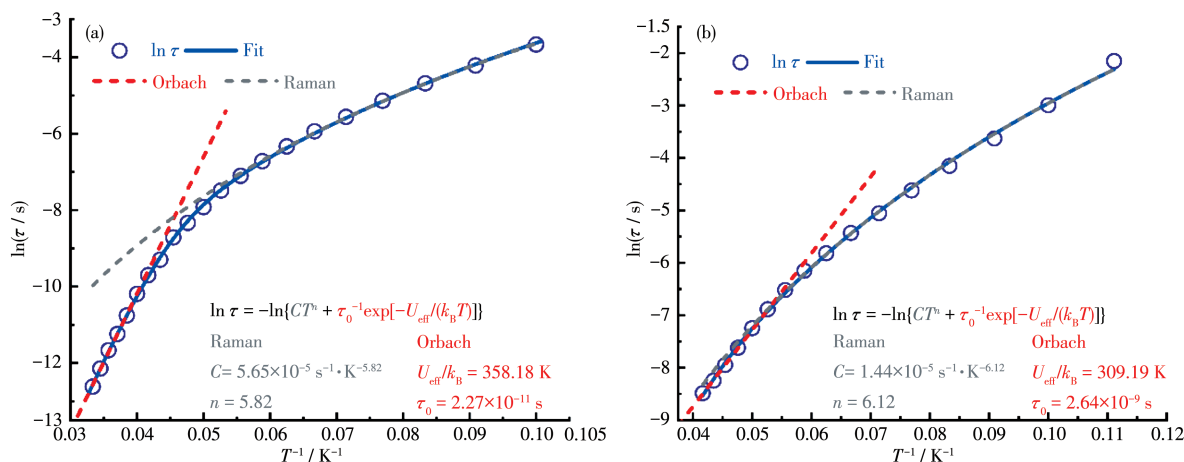


Fig.4 Cole-Cole plots of **1** (a) and **2** (b) with blue solid lines as Debye fits within indicated temperatures



Fig.5 Fitting of frequency-dependent of relaxation time of **1** (a) and **2** (b)

### 2.3 Structural correlation

Complexes **1** and **2** are actually analogous to each other but with different ac magnetic properties. Detailed insight into the structures of **1** and **2**, the axial O1—Dy1—O2 angle of 118.29° for complex **1** is larger than **2** of 115.26°. Meanwhile, the axial Dy1—O1 and Dy1—O2 average bond lengths in **1** (0.228 nm) are also slightly shorter than that detected in **2** (0.235 nm, Table 1). The presence of different counter anions ( $\text{ClO}_4^-$  and  $\text{CF}_3\text{SO}_4^-$ ) and solvent molecules ( $\text{CH}_3\text{OH}$ ,  $2\text{CH}_3\text{CN}$ ,  $2\text{H}_2\text{O}$  and  $2\text{CH}_3\text{OH}$ ,  $4\text{H}_2\text{O}$ ) of **1** and **2** in the crystal lattice results in slight structural changes and different Dy···Dy intermolecular interactions along *a*, *b*

and *c* axes (Fig.S2 and S3). The different intermolecular Dy···Dy interactions along *a*, *b* and *c* axes may bring different dipole-dipole interactions that are influencing on the relaxation rate of incoherent quantum tunneling of the magnetization to obtain different effective relaxation barriers. Collectively, the large angle and short bond lengths at the axial position incorporate with different intermolecular interactions in both the complexes may induce the stronger axial magnetic anisotropy which is mainly responsible for higher energy barrier of 358 K in **1** than that observed in complex **2** of 309 K.

Table 1 Important bond lengths (nm) and angles (°) of axially coordinated O of **L** for **1** and **2**

Complex	<b>1</b>		<b>2</b>	
Length / nm	Dy1—O1	0.223 3(3)	Dy1—O1	0.225 1(3)
	Dy1—O2	0.222 3(3)	Dy1—O2	0.221 9(3)
	average	0.228(3)	average	0.235(3)
Angle / (°)	O2—Dy1—O1	118.29(11)	O2—Dy1—O1	115.26(11)
$\tau_0$ / s	$2.27 \times 10^{-11}$		$2.64 \times 10^{-9}$	
$U_{\text{eff}}$ / K	358.18		309.19	

### 3 Conclusions

In summary, two new triaminoguanidine-based mononuclear Dy (III) complexes with formulas  $[\text{DyL}_2(\text{H}_2\text{O})_2]\text{ClO}_4 \cdot \text{solvent}$  (**1**) and  $[\text{DyL}_2(\text{H}_2\text{O})_2]\text{CF}_3\text{SO}_3 \cdot \text{solvent}$  (**2**) have been successfully prepared by altering the reaction conditions. Both the complexes display almost analogous structures featuring eight coordinated  $\text{N}_4\text{O}_4$  environment each that can be best described as triangular dodecahedron  $D_{2d}$  symmetry. The experimen-

tal ac magnetic studies revealed the single-ion magnetic behavior under zero dc applied field with effective energy barriers ( $U_{\text{eff}}$ ) of 358 K (**1**) and 309 K (**2**), respectively. The diverse ac magnetic behaviors may result from different types of lattice counter anions ( $\text{ClO}_4^-$  for **1** and  $\text{CF}_3\text{SO}_4^-$  for **2**), which slightly but significantly affect the axial ligand field parameters and coordination geometries. These results offer an interesting and possible opportunity for tuning the magnetic properties

of SIMs by affecting the axial ligand field through introducing different counter anions into the crystal lattice.

**Acknowledgments:** We thank the National Natural Science Foundation of China (Grants No.21871247, 21801237), the Natural Science Foundation of Jilin Province of China (Grant No. 20200201244JC) and Key Research Program of Frontier Sciences, CAS (Grant No. ZDBS-LY-SLH023) for financial support. ALI Basharat is grateful for the support through CAS-TWAS President's Fellowship.

**Conflicts of Interest:** The authors declare no conflict of interest.

Supporting information is available at <http://www.wjhxb.cn>

## References:

- [1] Bogani L, Wernsdorfer W. *Nat. Mater.*, **2008**, *7*(3):179-186
- [2] Rocha A R, Garcia-Suarez V M, Bailey S W, Lambert C J, Ferrer J, Sanvito S. *Nat. Mater.*, **2005**, *4*(4):335-339
- [3] Wernsdorfer W, Sessoli R. *Science*, **1999**, *284*(5411):133-135
- [4] Mannini M, Pineider F, Sainctavit P, Danieli C, Otero E, Sciancalepore C, Talarico A M, Arrio M A, Cornia A, Gatteschi D, Sessoli R. *Nat. Mater.*, **2009**, *8*(3):194-197
- [5] Wernsdorfer W. *C. R. Chim.*, **2008**, *11*(10):1086-1109
- [6] Moreno-Pineda E, Godfrin C, Balestro F, Wernsdorfer W, Ruben M. *Chem. Soc. Rev.*, **2018**, *47*(2):501-513
- [7] Zhu Z H, Guo M, Li X L, Tang J K. *Coord. Chem. Rev.*, **2019**, *378*:350-364
- [8] Long J, Guari Y, Ferreira R A S, Carlos L D, Larionova J. *Coord. Chem. Rev.*, **2018**, *363*:57-70
- [9] Bar A K, Pichon C, Sutter J P. *Coord. Chem. Rev.*, **2016**, *308*:346-380
- [10] Bar A K, Kalita P, Singh M K, Rajaraman G, Chandrasekhar V. *Coord. Chem. Rev.*, **2018**, *367*:163-216
- [11] Feng M, Tong M L. *Chem. Eur. J.*, **2018**, *24*(30):7574-7594
- [12] Craig G A, Murrie M. *Chem. Soc. Rev.*, **2015**, *44*(8):2135-2147
- [13] Day B M, Guo F S, Layfield R A. *Acc. Chem. Res.*, **2018**, *51*(8):1880-1889
- [14] Guo F S, Day B M, Chen Y C, Tong M L, Mansikkamaki A, Layfield R A. *Science*, **2018**, *362*(6421):1400-1403
- [15] Goodwin C A P, Ortu F, Reta D, Chilton N F, Mills D P. *Nature*, **2017**, *548*(7668):439-442
- [16] Guo F S, Day B M, Chen Y C, Tong M L, Mansikkamaki A, Layfield R A. *Angew. Chem. Int. Ed.*, **2017**, *56*(38):11445-11449
- [17] Meng Y S, Jiang S D, Wang B W, Gao S. *Acc. Chem. Res.*, **2016**, *49*(11):2381-2389
- [18] Cen P P, Zhang S, Liu X Y, Song W M, Zhang Y Q, Xie G, Chen S P. *Inorg. Chem.*, **2017**, *56*(6):3644-3656
- [19] Liu X Y, Li F F, Ma X H, Cen P P, Luo S C, Shi Q, Ma S R, Wu Y W, Zhang C C, Xu Z, Song W M, Xie G, Chen S P. *Dalton Trans.*, **2017**, *46*(4):1207-1217
- [20] Zhang X J, Vieru V, Feng X W, Liu J L, Zhang Z J, Na B, Shi W, Wang B W, Powell A K, Chibotaru L F, Gao S, Cheng P, Long J R. *Angew. Chem. Int. Ed.*, **2015**, *54*(34):9861-9865
- [21] Liu S T, Lu J J, Li X L, Zhu Z H, Tang J K. *Dalton Trans.*, **2020**, *49*(35):12372-12379
- [22] Canaj A B, Dey S, Mart E R, Wilson C, Rajaraman G, Murrie M. *Angew. Chem. Int. Ed.*, **2019**, *58*(40):14146-14151
- [23] Jiang X J, Li M, Lu H L, Xu L H, Xu H, Zang S Q, Tang M S, Hou H W, Mak T C W. *Inorg. Chem.*, **2014**, *53*(24):12665-12667
- [24] Müller I M, Möller D. *Eur. J. Inorg. Chem.*, **2005**(2):257-263
- [25] Müller I M, Spillmann S, Franck H, Pietschnig R. *Chem. Eur. J.*, **2004**, *10*(9):2207-2213
- [26] Müller I M, Möller D, Föcker K. *Chem. Eur. J.*, **2005**, *11*(11):3318-3324
- [27] Oppel I M, Föcker K. *Angew. Chem. Int. Ed.*, **2008**, *47*(2):402-405
- [28] Müller I M, Robson R, Separovic F. *Angew. Chem. Int. Ed.*, **2001**, *40*(23):4385-4386
- [29] Müller I M, Robson R. *Angew. Chem. Int. Ed.*, **2000**, *39*(23):4357-4359
- [30] Conerney B, Jensen P, Kruger P E, MacGloinn C. *Chem. Commun.*, **2003**, *11*:1274-1275
- [31] Kisets I, Gelman D. *Organometallics*, **2018**, *37*(4):526-529
- [32] Lusby P J, Mueller P, Pike S J, Slawin A M Z. *J. Am. Chem. Soc.*, **2009**, *131*(45):16398-16400
- [33] Liu Y, Xuan W M, Zhang H, Cui Y. *Inorg. Chem.*, **2009**, *48*(21):10018-10023
- [34] Plass W. *Coord. Chem. Rev.*, **2009**, *253*(19/20):2286-2295
- [35] Böhme M, Ion A E, Kintzel B, Buchholz A, Görls H, Plass W. *Z. Anorg. Allg. Chem.*, **2020**, *646*(13):999-1009
- [36] Zharkouskaya A, Görls H, Vaughan G, Plass W. *Inorg. Chem. Commun.*, **2005**, *8*(12):1145-1148
- [37] Zharkouskaya A, Buchholz A, Plass W. *Eur. J. Inorg. Chem.*, **2005**(24):4875-4879
- [38] Plaul D, Boehme M, Ostrovsky S, Tomkowicz Z, Goerls H, Haase W, Plass W. *Inorg. Chem.*, **2018**, *57*(1):106-119
- [39] Böhme M, Schuch D, Buchholz A, Görls H, Plass W. *Z. Anorg. Allg. Chem.*, **2020**, *646*(3):166-174
- [40] Hamblin J, Tuna F, Bunce S, Childs L J, Jackson A, Errington W, Alcock N W, Nierengarten H, Van Dorselaer A, Leize-Wagner E, Hannon M J. *Chem. Eur. J.*, **2007**, *13*(33):9286-9296
- [41] Spielberg E T, Gilb A, Plaul D, Geibig D, Hornig D, Schuch D, Buchholz A, Ardavan A, Plass W. *Inorg. Chem.*, **2015**, *54*(7):3432-3438
- [42] Kintzel B, Boehme M, Liu J J, Burkhardt A, Mrozek J, Buchholz A, Ardavan A, Plass W. *Chem. Commun.*, **2018**, *54*(92):12934-12937
- [43] Liu J J, Mrozek J, Myers W K, Timco G A, Winpenny R E P, Kintzel B, Plass W, Ardavan A. *Phys. Rev. Lett.*, **2019**, *122*(3):037202
- [44] Ali B, Gendron F, Li X L, Le Guennic B, Tang J K. *Chem*, **2020**, *4*:4
- [45] Ali B, Li X L, Gendron F, Le Guennic B, Tang J K. *Dalton Trans.*,

- 2021,50**(15):5146-5153
- [46]Ion A E, Spielberg E T, Görls H, Plass W. *Inorg. Chim. Acta*, **2007**, **360**(13):3925-3931
- [47]Winkelmann E, Raether W. *Chem. Abstr.*, **1972**:126264
- [48]Bain G A, Berry J F. *J. Chem. Educ.*, **2008,85**(4):532-536
- [49]Sheldrick G M. *Acta Crystallogr. Sect. A*, **2015,A71**:3-8
- [50]Sheldrick G M. *Acta Crystallogr. Sect. C*, **2015,C71**:3-8
- [51]Zabrodsky H, Peleg S, Avnir D. *J. Am. Chem. Soc.*, **1993,115**(18): 8278-8289
- [52]Alvarez S, Alemany P, Casanova D, Cirera J, Llunell M, Avnir D. *Coord. Chem. Rev.*, **2005,249**(17):1693-1708
- [53]Ruiz-Martínez A, Casanova D, Alvarez S. *Chem. Eur. J.*, **2008,14**(4): 1291-1303
- [54]Zhang S, Mo W J, Zhang J W, Zhang Z Q, Yin B, Hu D W, Chen S P. *Inorg. Chem.*, **2019,58**(22):15330-15343
- [55]Tang J K, Hewitt I, Madhu N T, Chastanet G, Wernsdorfer W, Anson C E, Benelli C, Sessoli R, Powell A K. *Angew. Chem. Int. Ed.*, **2006**, **45**(11):1729-1733
- [56]Zhang P, Zhang L, Wang C, Xue S F, Lin S Y, Tang J K. *J. Am. Chem. Soc.*, **2014,136**(12):4484-4487
- [57]Liu X Y, Ma X F, Yuan W Z, Cen P P, Zhang Y Q, Ferrando-Soria J, Xie G, Chen S P, Pardo E. *Inorg. Chem.*, **2018,57**(23):14843-14851
- [58]Ma X F, Chen B B, Zhang Y Q, Yang J H, Shi Q, Ma Y L, Liu X Y. *Dalton Trans.*, **2019,48**(33):12622-12631
- [59]Gao Y J, Xu G F, Zhao L, Tang J K, Liu Z L. *Inorg. Chem.*, **2009,48** (24):11495-11497